

Article

# Mathematical Perspectives in the Variable Texture Products Cutting Process

Mirela Panainte-Lehăduș <sup>1</sup>, Emilian Moșneguțu <sup>1,\*</sup>, Narcis Bârsan <sup>1</sup>, Gabriela Andrioai <sup>2</sup>,  
Claudia Tomozei <sup>1,\*</sup> and Oana Irimia <sup>1</sup>

<sup>1</sup> Department of Environmental Engineering and Mechanical Engineering, Faculty of Engineering, Vasile Alecsandri University of Bacau, 157 Calea Marasesti, 600115 Bacau, Romania

<sup>2</sup> Department of Foreign Languages and Literature, Faculty of Letters, Vasile Alecsandri University of Bacau, 157 Calea Marasesti, 600115 Bacau, Romania

\* Correspondence: emos@ub.ro (E.M.); claudia.tomozei@ub.ro (C.T.)

**Abstract:** The methods utilized to construct and identify the mathematical equation that characterizes the cutting of items with varied textures are presented in this work. Using laboratory equipment, the cutting process was carried out experimentally. The cutting energy was calculated based on the experimental results. The energy required to perform this process is directly influenced by the textural characteristics of the products used, as per the analysis of the experimental results obtained after the cutting process (density, humidity, products with or without peel). The gathered information was used to develop a general equation that would properly describe the process. Table Curve 3D software was used to create mathematical equations that define the relationship between input parameters, the type of product being cut, cutting speed, and output parameters, i.e., cutting energy. The equations that have the same correlation coefficient were discovered using the working methodology; it was specifically designed for this purpose.

**Keywords:** mathematical equations; products texture; cutting process; cutting energy



**Citation:** Panainte-Lehăduș, M.; Moșneguțu, E.; Bârsan, N.; Andrioai, G.; Tomozei, C.; Irimia, O. Mathematical Perspectives in the Variable Texture Products Cutting Process. *Processes* **2022**, *10*, 1603. <https://doi.org/10.3390/pr10081603>

Academic Editors: Vlad Mureșan and Adriana Paucean

Received: 25 July 2022

Accepted: 10 August 2022

Published: 13 August 2022

**Publisher's Note:** MDPI stays neutral with regard to jurisdictional claims in published maps and institutional affiliations.



**Copyright:** © 2022 by the authors. Licensee MDPI, Basel, Switzerland. This article is an open access article distributed under the terms and conditions of the Creative Commons Attribution (CC BY) license (<https://creativecommons.org/licenses/by/4.0/>).

## 1. Introduction

Because agri-food products are varied and have characteristics that change over time and location, cutting them is a highly difficult task.

Cutting solid materials is common and important due to the large quantities of raw materials and processed products, as well as the energy consumption, of which only a small fraction (0.1–0.2%) is used to overcome the cohesive forces in the particles, with the rest dissipating unnecessarily and even harmfully in the form of heat [1–3].

Prior to determining the conditions under which the cutting process will be carried out with maximum efficiency, it is necessary to have a solid understanding of the characteristic indices of the products to be cut (raw material properties, required quality conditions, properties related to the texture of the products to be shredded), as well as their effect on the cutting process. Many specialized studies have shown that as moisture content increased, so did specific energy consumption [4–6].

Particle cutting requires a certain amount of energy. The specific energy consumption (J/kg) in the cutting process reflects the amount of energy required to achieve a specified degree of cutting off the unit mass of the product under cut [2,3,7]. The nature of the material being ground, its initial state, structure, and internal condition, the size, speed, and duration of the mechanical stress applied, the nature of the forces applied, the particle size before and after cutting, and the cutting degree are all factors that affect this process [8–13].

The energy consumed during the cutting process is only partially usable; the remainder goes to the development of elastic and plastic deformations in the cutting material, particle friction between themselves and the machine's active organs, and internal mechanical losses [8,14–18].

Cutting is an inefficient process in terms of energy consumption. There is no clear method of calculating the minimum amount of energy necessary for cutting, however, numerous hypotheses have been proposed [16–20].

Many of the equations for calculating cutting energy that has been developed in the literature are empirical [1,3,9,10]. The three cutting equations that exist in the literature are based on a hypothesis that has received a lot of attention in the literature [8,15,17,18,20–24].

Bond correlates the energy for shredding to the size of a single particle. According to Kick, the energy of the particles is proportionate to their volume [17,18]. Rittinger believes that the amount of energy spent during the cutting process is proportionate to the new surface formed throughout the cutting process [1,3,17,18,21,23,24]. Each of the three equations has a specific constant, the value of which must be calculated from experimental data. The following is how Rittinger's connection for agri-food items with a variable texture was employed in this study:

$$E_R = k_R \left( \frac{1}{d} - \frac{1}{D} \right) \quad (1)$$

in which:  $D$  is the average size of the material to be cut;  $d$  is the average size of the cutting material;  $k_R$  is Rittinger's constant, considered as:

$$k_R = F_m \cdot S_n \quad (2)$$

where:  $F_m$  is the cutting force,  $S_n$  is the new surface created.

The next stage in working with experimental data, according to the literature, is to identify the mathematical equations that describe the correlations between the input and tracked parameters [25–34].

In the specialized literature, there are a lot of experiments that deal with the cutting process and the identification of the mathematical equations that describe this process. However, these equations are generated for specific cases. In conclusion, the purpose of this paper was to develop a general equation that described the relationships between the operating parameters of the cutting equipment and the energy required to fulfill the process (value defined by relation (1)). The mathematical equations that have been chosen to describe the cutting process have resulted from a methodology that can give the equations obtained a general character. An approach for processing the set of equations generated by Table Curve 3d software was created and designed for this purpose [35].

## 2. Materials and Methods

The investigation was conducted using a texture analyzer to determine the energy required to accomplish the cutting operation for various products. Texture Profile Analysis (TPA) is an objective method of sensory analysis developed by Szczesniak in 1963. He was the first to specify the textural parameters for this method. This method (Texture Profile Analysis-TPA) is based on the concept that texture is a highly influenced characteristic by a variety of factors [3,17,18,21,23,24].

The "Texture Analyzer-TA-XT2i" measurement equipment is used for this (Figure 1a,b) because it gives a three-dimensional study of the cutting force based on the knife's stroke during the cutting process and the cutting time.

Cohesion, reliability, elasticity, freshness, breaking strength, penetration strength, expansion strength, adhesiveness, ability to masticate, and other tests may be assessed using the device and the "Texture Expert" application [14,16–18]. As a cutting device, the sample type HDP/BS was used in this investigation (Figure 1b,c).

Different species and varieties of vegetables and fruits were chosen to represent a wide variety of vegetable items with a texture liked by the descriptor "hard" in order to carry out the study regarding the process of cutting experiments. The species and varieties for which the determinations were performed are shown in Tables 1 and 2.

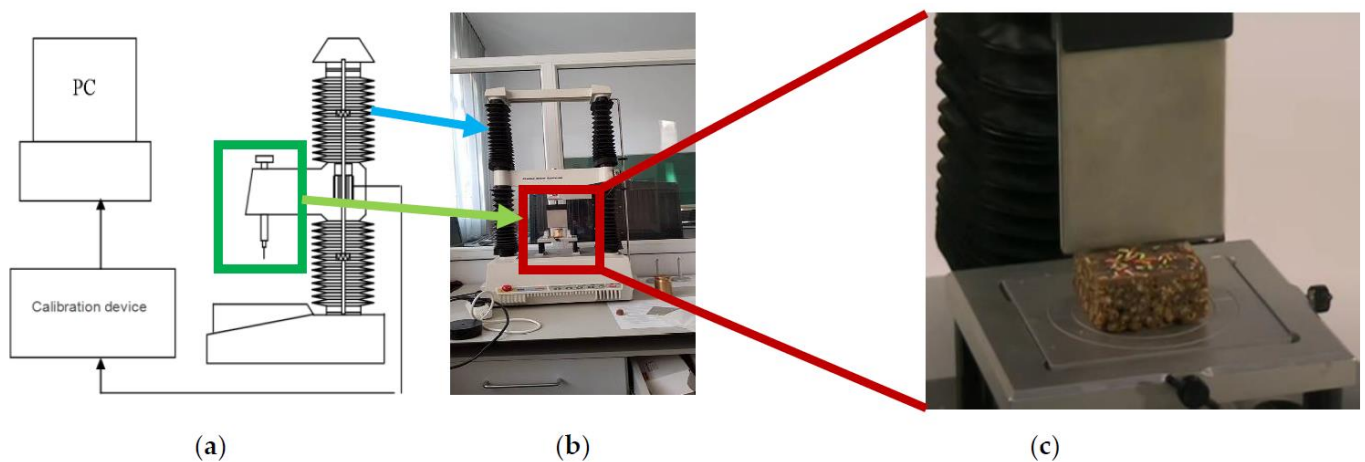


**Figure 1.** Texture Analyser-TA-XT2i [36]: (a) the analyzer’s technical system; (b) an image of the device in operation; (c) the cutting device.

**Table 1.** Texture analysis was conducted to analyze various fruit species and varieties [22].

Item No.	Species	Variety	Maturity	Observation
1.	Apple	Grave Steiner	Complete	Unpeeled
2.	Apple	Grave Steiner	Complete	Peeled
3.	Apple	Ida Red	Complete	Unpeeled
4.	Apple	Ida Red	Complete	Peeled
5.	Apple	Golden Delicious	Complete	Unpeeled
6.	Apple	Golden Delicious	Complete	Peeled
7.	Apple	Jonagold	Complete	Unpeeled
8.	Apple	Jonagold	Complete	Peeled
9.	Pear	Clapp’s Favorite	Ripen	Unpeeled
10.	Pear	Clapp’s Favorite	Ripen	Peeled

**Table 2.** Vegetable species and varieties analyzed by the method of texture analysis [22].

Item No.	Species	Variety	Maturity	Observation
1.	Potato	Désirée	Complete	Unpeeled
2.	Potato	Désirée	Complete	Unpeeled
3.	Potato	Sante	Complete	Unpeeled
4.	Potato	Sante	Complete	Peeled
5.	Carrot	Nassan	Complete	Unpeeled
6.	Carrot	Nassan	Complete	Peeled
7.	Celery	Victoria	Complete	Unpeeled
8.	Celery	Victoria	Complete	Peeled
9.	Parsnip	Long White	Complete	Unpeeled
10.	Parsnip	Long White	Complete	Peeled

The parameters of the investigated products vary depending on the species and variety. Tables 3 and 4 show the average humidity and density for the investigated varieties.

**Table 3.** The average density and average humidity of the fruits that have been analyzed [22].

Item No.	Species	Density (kg/m <sup>3</sup> )	Humidity (%)
1.		790	88.5
2.		846	87.5
3.	Apple	920	84.1
4.		930	83.5
5.	Pear	1028	85.1

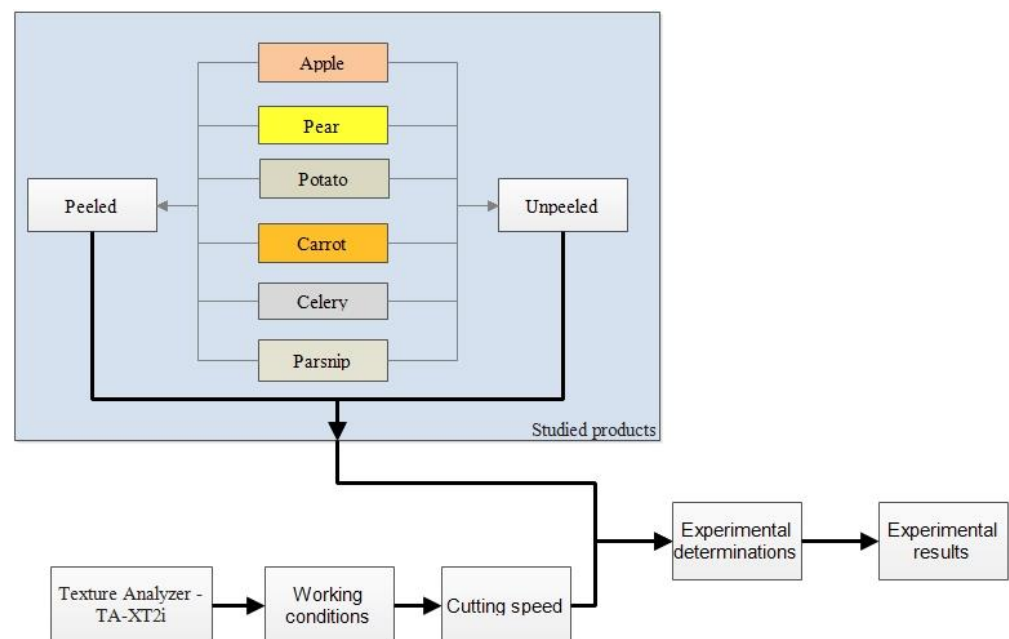
**Table 4.** The average density and average humidity of the vegetables were investigated [22].

Item No.	Species	Density (kg/m <sup>3</sup> )	Humidity (%)
1.		1010	82.3
2.	Potato	1050	74.5
3.		1060	79.6
4.	Carrot	1040	88.8
5.	Celery	964	87.0
6.	Parsnip	994	89.5

The following conclusions can be derived from the examination of the parameters that characterize the products that will be subjected to the analysis:

- The variation of their density is inversely proportional to the variation of the humidity in the case of the apple product used in these experimental determinations;
- In the case of the potato product, it was found that the lowest product density is associated with the highest humidity. The lowest value of the parameter studied was obtained for the next value of the density of the studied product, and for the highest value of the density, it was found that the humidity is higher by 5.1% compared to the minimum value;
- Because we only have one sample of the other products used in the study, no relevant conclusions can be drawn.

The investigations were carried out in accordance with the working technique represented in Figure 2.

**Figure 2.** For experimental determinations, there is a working methodology.

### 3. Results

Following the replacement of the experimental results obtained under Equation (1), a series of cutting energy values were produced, which are represented graphically in Figures 3–10.

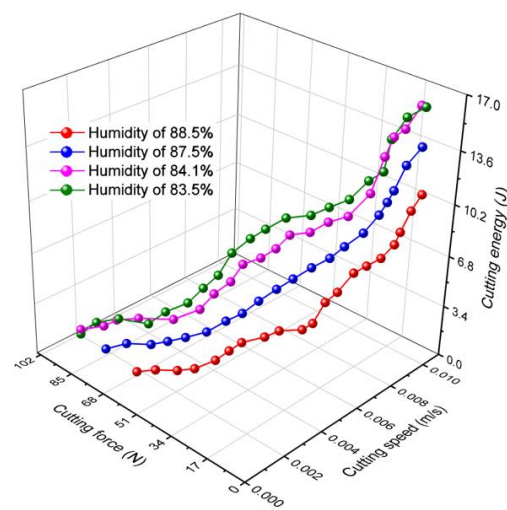


**Figure 3.** Variation in cutting energy for unpeeled apples with different humidity levels based on cutting speed.

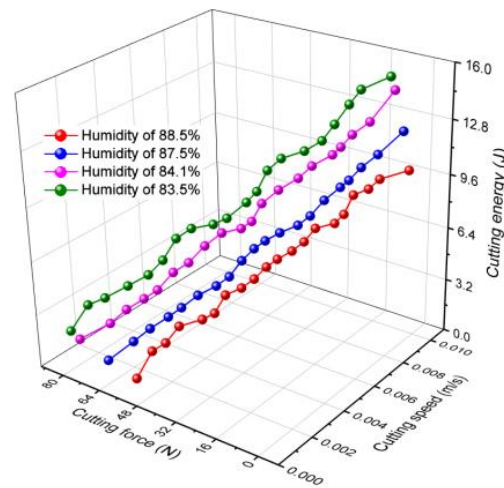


**Figure 4.** Variation in cutting energy for peeled apples with different humidity levels as a function of cutting speed.

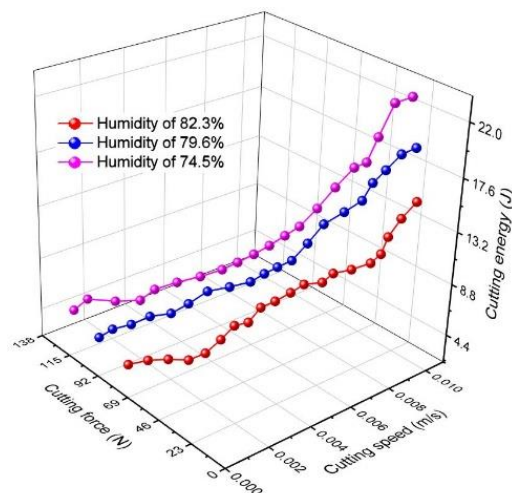


**Figure 5.** Variation in cutting energy for unpeeled potatoes with different humidity levels as a function of cutting speed.

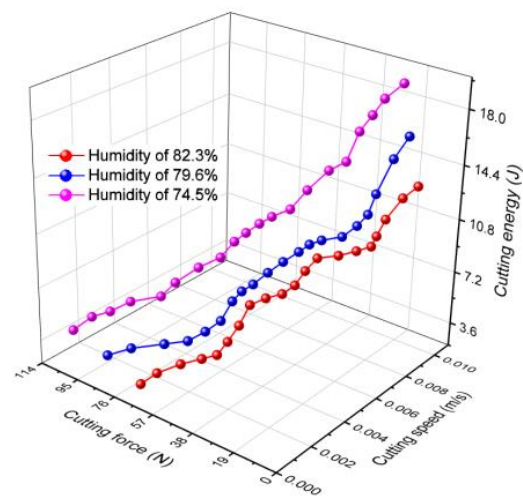


**Figure 6.** Variation in cutting energy for peeled potatoes with different humidity levels as a function of cutting speed.

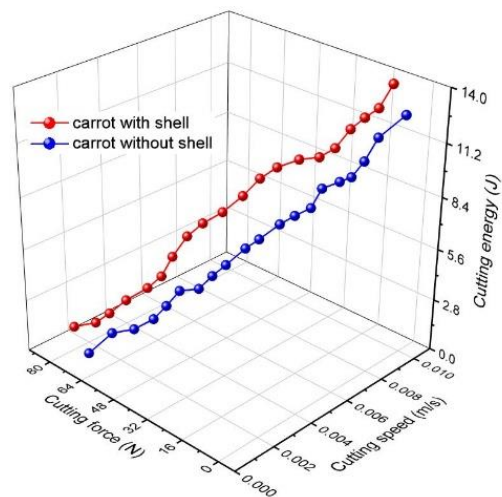


**Figure 7.** Variation in cutting energy for peeled and unpeeled carrots with different humidity levels as a function of cutting speed.

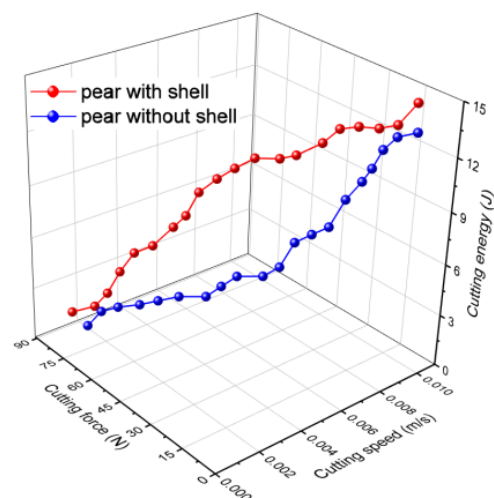


**Figure 8.** Variation in cutting energy for peeled and unpeeled pears with different humidity levels as a function of cutting speed.

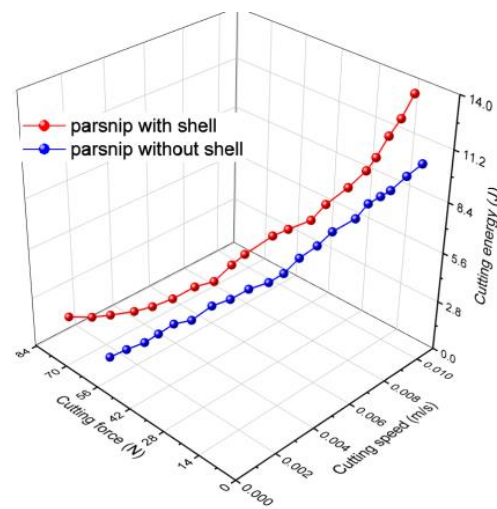


**Figure 9.** Variation in cutting energy for peeled and unpeeled parsnip with different humidity levels as a function of cutting speed.

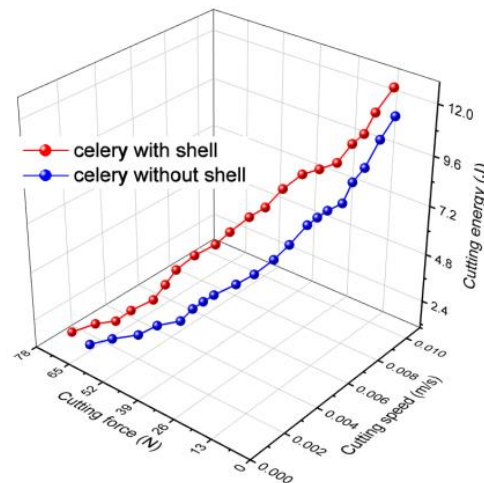


**Figure 10.** Variation in cutting energy for peeled and unpeeled celery with different humidity levels as a function of cutting speed.

The study of the results obtained by using the texture analysis approach to determine the cutting energy reveals that:

- the textural properties of the products to be cut (humidity of the products) influence the cutting process; high cutting energy values have been obtained for products with low humidity;
- The condition of the products to be cut has an impact on the cutting energy. According to the results of the experiments, when cutting unpeeled products, higher values of cutting energy were achieved than when cutting peeled products;
- The condition of the products being cut affects the cutting energy. When examining the obtained data, it is evident that there are small variations in cutting energy for small values of cutting speed, which can be seen when comparing unpeeled and peeled products, suggesting that the cutting energy for the same products tends to increase in direct proportion to the cutting speed. This is also confirmed by numerous field research, such as in the case of wheat straw cutting [7];
- Within the same species, cutting energy varies depending on variety, with the difference being mostly attributable to the textural characteristics, as shown in the case of celery, which has the biggest range of cutting energy observed, with its structure changing from the outside to the inside.

#### 4. Generating Mathematical Equations

The values obtained and represented in Figures 3–10 were used to determine the correlations between the current study’s input parameters (cutting speed and cutting force) and the output parameters (cutting energy).

Given its ability to generate over 30,000 types of equations, Table Curve 3D software was utilized to obtain these relationships [37].

The following are the actions that were taken in order to determine the mathematical equations that corresponded to the study that was conducted (Figure 11):

1. The experimental values obtained are inserted into an excel file, and the data are arranged in separate columns;
2. Table Curve 3D program allows the insertion of this excel file carrying data;
3. The parameters corresponding to the three axes are selected where, on the OX (cutting speed) and OY (cutting force) axes, the input parameters are introduced, while on the OZ (cutting energy) axis the tracked parameter is introduced;
4. Table Curve 3D software can generate equations that correlate to the values entered.
5. Following the equations generated by Table Curve 3D software, a total of 5198 equations was generated, which were organized as follows: (Figure 12):

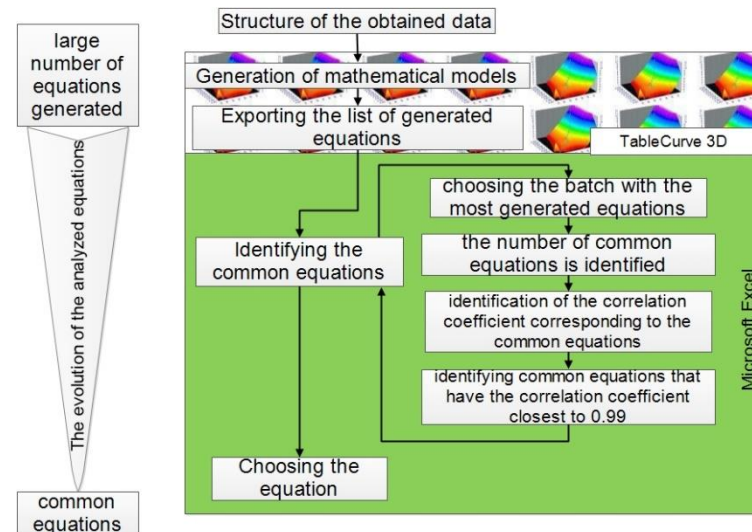


Figure 11. Identifying common equations: a working methodology.

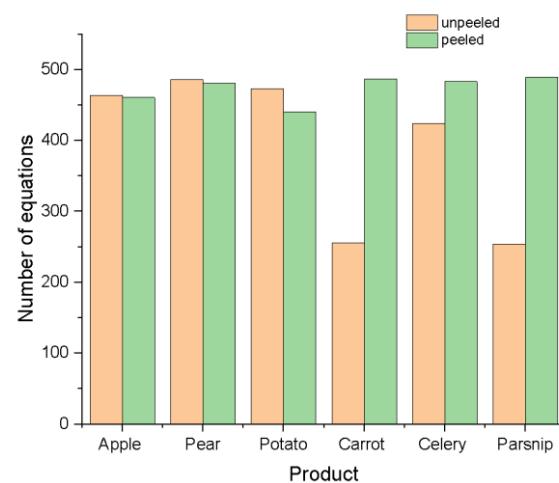
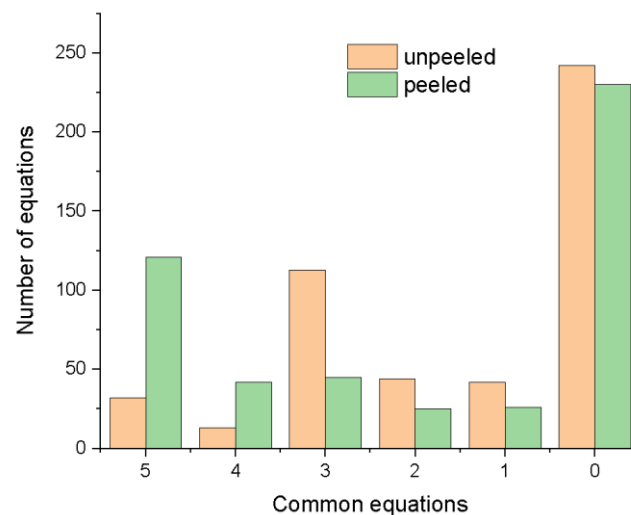


Figure 12. The number of equations generated by Table Curve 3d software varies according to the type of product under research.

- 2357 for products that have not been peeled;
- 2841 is the number for peeled products.

Table Curve 3D program has a database of these equations, each of which may be recognized by a number, in order to find the common equations.

6. A selection of common equations has been presented based on this facility, as follows:
  - A number of equations were generated for each group of experiments (with or without a peel) and for each sample in turn (apple, pear, potato, carrot, celery, and parsnip);
  - Within each experimental group (shell products—group a; peeled products—group b), a set of equations with the highest number of equations was chosen in comparison to the equations generated for the other samples (in our situation, we selected 486 equations for group A to correspond to the pear product and 489 equations for group B to correspond to the parsnip product);
  - In relation to this lot, similar equations (i.e., equations with the same identification number) have been identified, providing for preliminary filtering of the equations. The number of similar equations obtained from the study is shown in Figure 13. The number of similar equations identified in relation to the equations of the chosen reference lot is represented by numbers such as 5, 4, 3, 2, 1, and 0. (the lot with the most equations) (5—the equation is the same for all products; 0—the equation is unique to each product).



**Figure 13.** The number of common equations is represented graphically.

7. Figure 13 shows the common equations, which are defined by distinct correlation coefficients, and are seen in Figures 14 and 15 for each experimental sample. From the analysis of the graphical representations, it can be said:
  - for unpeeled products, the number of common equations was 32;
  - for peeled products, the number of common equations was 121;
  - Analyzing the distribution of the number of equations whose correlation coefficient is greater than 0.95 reveals:
    - In the case of unpeeled products, the highest number of equations was obtained for celery (32), followed by pear, parsnip, carrot, and apple, and the lowest number of equations was obtained for potato;
    - In the case of peeled products, the highest number of equations was obtained for celery (121), followed by parsnip, carrot, pear, and apple, and the lowest number of equations was obtained for potato.

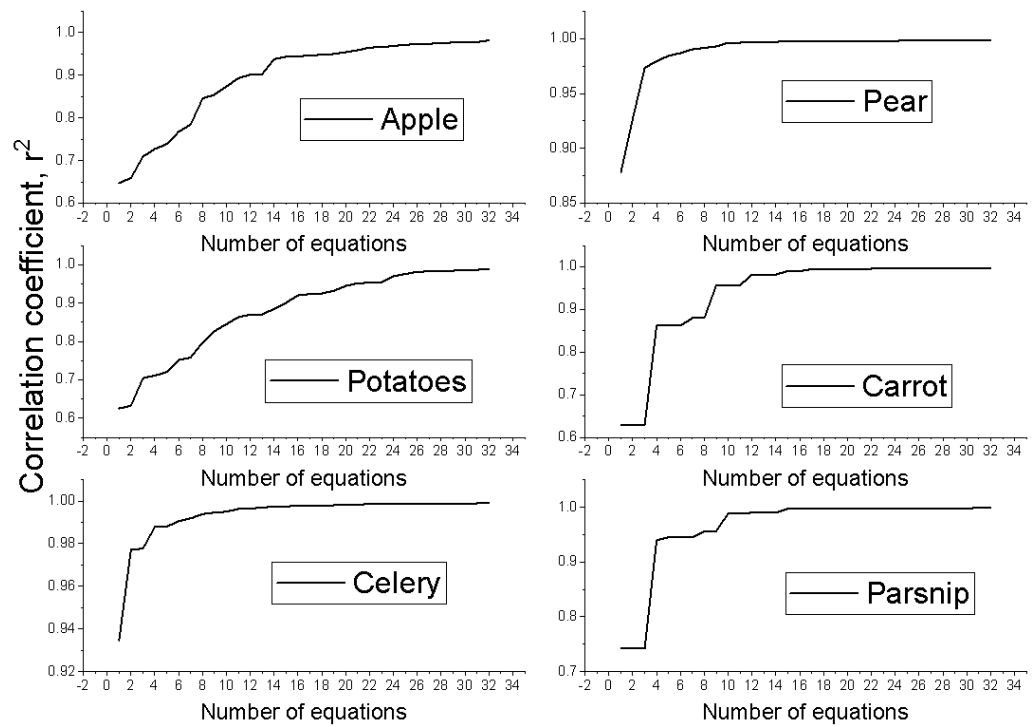


Figure 14. Variation of correlation coefficients for unpeeled products corresponding to common equations.

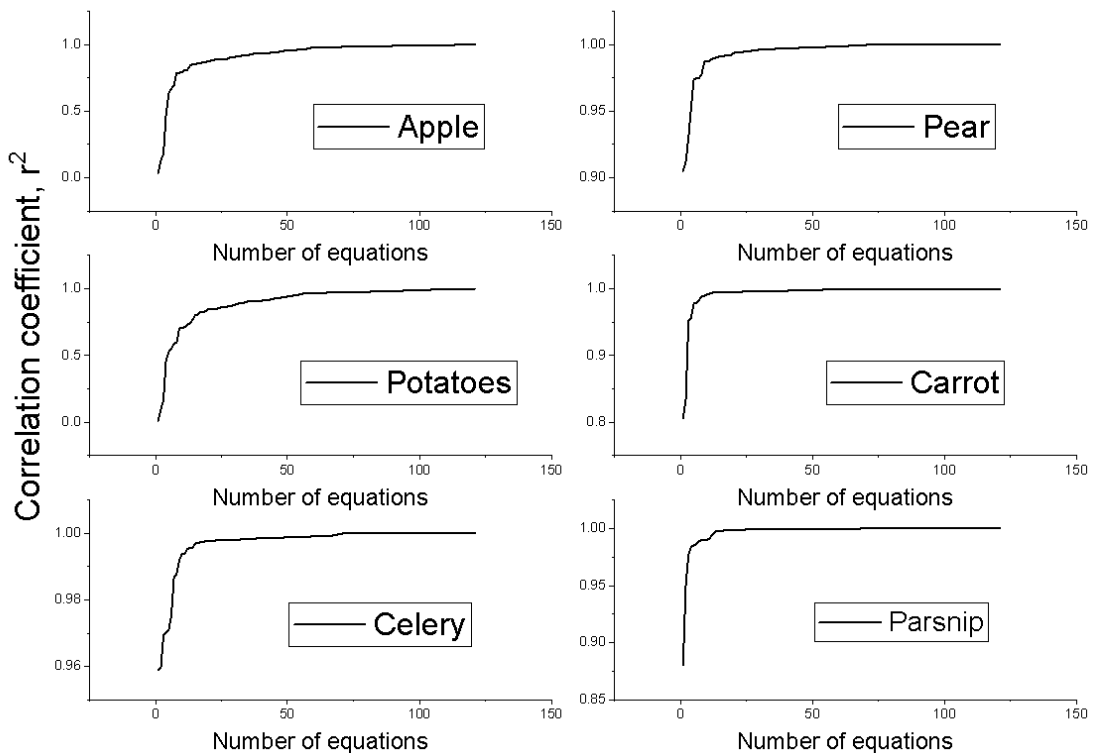
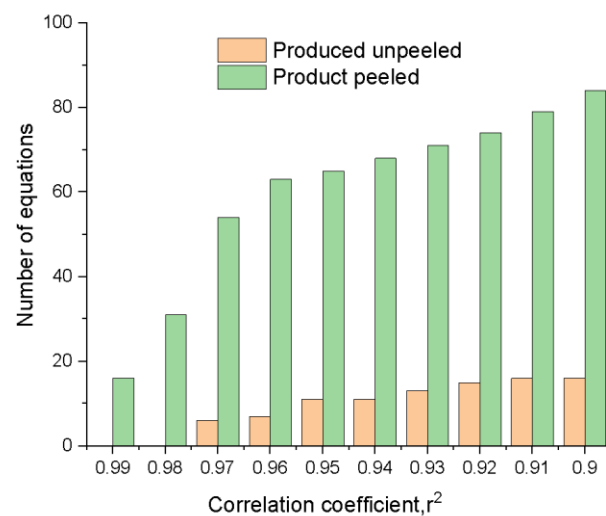


Figure 15. Variation of correlation coefficients for peeling products corresponding to common equations.

8. As previously stated, our goal was to find a common equation, therefore we searched over the results more than once to identify the equations with the correlation coefficient,  $r^2$ , which were closest to 0.99. In conclusion, for the range of values of the correlation coefficient  $r^2$  between 0.9 and 0.99, the number of equations available for solving the desired requirement has been graphically represented in Figure 16.



**Figure 16.** The correlation coefficient is used to represent the number of common equations.

9. The evaluation of a group of common equations based on the value of the correlation coefficient  $r^2$  has been the next step. At this moment, the common equations were created to have the same correlation coefficient value. Followed by an analysis of the correlation coefficients corresponding to the common equations, a total of 6 equations for an  $r^2$  high of 0.97 have been discovered for the experimental batches of peeled products, and a number of 54 equations for the experimental group of unpeeled products.

The goal of this study was to find the common equations that describe the cutting process for diverse materials for both peeled and unpeeled products. The remaining equations (6 equations for peeled products and 54 equations for unpeeled products) were then analyzed for this purpose, revealing 4 main equations. These four final equations are put through a visual inspection, with the value of the terms of the equations compared to the described equations. This is required if indeed the mathematical model chosen has to be confirmed.

10. When the values of the terms of the equation generated by the Table Curve 3D software are examined, it is discovered that some equation terms have a value bigger than  $e^{+8}$ , meaning a thorough identification of the relevant term is difficult (since the entire value of the terms is necessary for the validation of the model). Following such an examination, only two possible equations remained out of the four common equations, whose model, in our situation, is provided by the logarithmic equations shown in Equations (3) and (4) (corresponding to equation number 145 and equation number 150—from the Table Curve 3D software database).

$$z = a + b \cdot \ln x + c \cdot (\ln x)^2 + d \cdot (\ln x)^3 + e \cdot (\ln x)^4 + f \cdot (\ln x)^5 + g \cdot \ln y + h \cdot (\ln y)^2 + i \cdot (\ln y)^3 + j \cdot (\ln y)^4 + k \cdot (\ln y)^5 \quad (3)$$

$$z = a + b \cdot \ln x + c \cdot (\ln x)^2 + d \cdot (\ln x)^3 + e \cdot (\ln x)^4 + f \cdot (\ln x)^5 + \frac{g}{y} + \frac{h}{y^2} + \frac{i}{y^3} + \frac{j}{y^4} + \frac{k}{y^5} \quad (4)$$

After analyzing the work steps presented above, a graphical representation (Figure 17) was created to highlight the methodology for identifying a general equation to determine the energy required to cut different agri-food products, depending on the speed of the cutting device and the force used to carry out this process. Figure 17 shows the whole methodology for choosing the mathematical equation that explains this procedure, and it is valid for peeled products that have been subjected to experimental determinations (for unpeeled products, the representation is approximately identical).

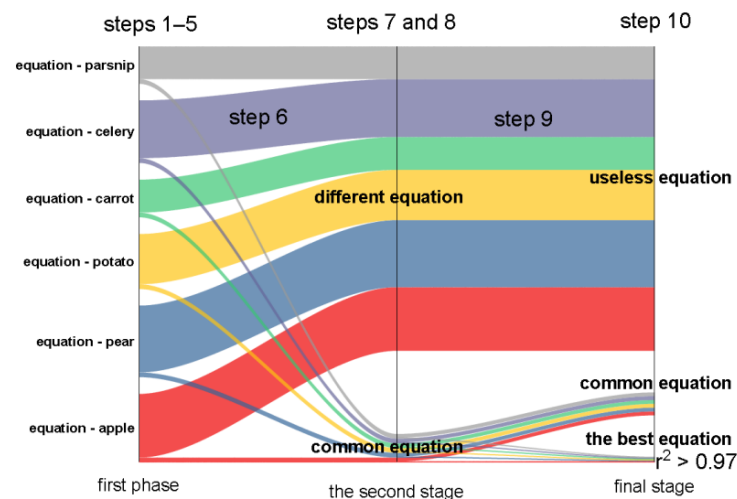


Figure 17. Working steps for choosing the common mathematical equation.

Figure 18 illustrates the response area created by the Table Curve 3D software in the example of the peeled apple product for equation no. 145.

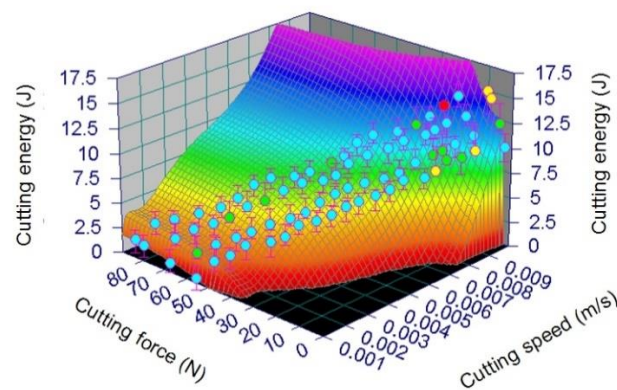


Figure 18. The surface generated by equation no. 145 for peeled apples.

## 5. Conclusions

The following conclusions may be taken from the examination of the obtained data:

- A number of agri-food products (fruit-apple, pear; root-potato, carrot, celery, and parsnip), peeled or unshelled, were used to determine the energy required for cutting vegetable products;
- Only the density and humidity of the products used could be noted because of the diversity of the chosen products. Taking it into account, the apple has the lowest density ( $790 \text{ kg/m}^3$ ), while the potato has the highest density ( $1060 \text{ kg/m}^3$ ). When it regards humidity, potatoes have the lowest humidity (74.5%), and parsnips have the highest (89.5%);
- The cutting process is influenced directly by the textural properties of the products used in these experimental evaluations:
- The highest value of energy used to carry out the cutting process was obtained for the product with the lowest humidity, the peeled potato, whose humidity was 74.5% and 23.16 J, respectively, and the lowest value was obtained for unpeeled celery, respectively 11.44 J.
- In regard to the humidity characteristic, it can be said that it has a direct and inversely proportional influence on the cutting energy value;
- In terms of product character, both peeled and unpeeled, it is discovered that the energy required to cut peeled products is more than the energy necessary to cut unpeeled products, regardless of the type of the product used;

- When the energy required to carry out the cutting process is examined in relation to the force used and the cutting device's speed of movement, it is discovered that these characteristics have a direct impact on the parameter analyzed, independently of the type of the product used;
- Using the Table Curve 3D software, the obtained data were utilized to produce mathematical equations;
- An analysis methodology has been developed to identify a common equation for all experimental groups, which can be generalized to other types of experiments as well;
- Following the working stages of the experimental data, it is found that:
  - For peeled products, where a total of 2357 equations were created, 32 common equations were generated, only 6 of which satisfied the criterion of  $r^2$  being larger than 0.97;
  - For unpeeled products, it resulted in a total of 2841 equations, 121 of which were common and 54 of which satisfied the requirement of  $r^2$  having larger than 0.97;
  - Following a visual examination of the Table Curve 3D program's mathematical equations, which satisfied the two primary requirements:
    - To have an  $r^2 >$  of 0.97 (6 equations for peeled products and 54 for unpeeled products);
    - To have something in common with both peeled and unpeeled products;
    - We had the option of choosing between two logarithmic equations;
- Two common logarithmic equations describing the dependency between the cutting energy required to cut different types of products (peeled and/or unpeeled) depending on the cutting speed and force, and the dependency characteristic of the cutting process of hard-textured products, were identified following the analysis of the equations obtained using the Table Curve 3D software.

**Author Contributions:** Conceptualization, M.P.-L. and E.M.; methodology, E.M.; software, E.M.; validation, N.B.; formal analysis, C.T.; investigation, O.I.; resources, M.P.-L.; data curation, M.P.-L.; writing—original draft preparation, M.P.-L. and E.M.; writing—review and editing, G.A.; visualization, C.T.; supervision, N.B. All authors have read and agreed to the published version of the manuscript.

**Funding:** This research received no external funding.

**Institutional Review Board Statement:** Not applicable.

**Informed Consent Statement:** Not applicable.

**Data Availability Statement:** Not applicable.

**Conflicts of Interest:** The authors declare no conflict of interest.

## References

1. Earle, R.L. *Unit Operations in Food Industry*; The New Zealand Institute of Food Science and Technology: Palmerston North, New Zealand, 1983.
2. Mohsenin, N.N. *Physical Properties of Plant and Animal Materials*; Gordon and Breach Science Publishers: New York, NY, USA, 1970.
3. Bourne, M.C. *Basic Principles of Food Texture Measurement*; Lecture text of Dough Rheology and Baked Products Texture Workshop: Chicago, IL, USA, 1988.
4. Mani, S.; Tabil, L.G.; Sokhansanj, S. Grinding performance and physical properties of wheat and barley straws, corn stover and switchgrass. *Biomass Bioenergy* **2004**, *27*, 339–352. [[CrossRef](#)]
5. Tumuluru, J.S.; Tabil, L.G.; Song, Y.; Iroba, K.L.; Meda, V. Grinding energy and physical properties of chopped and hammer-milled barley, wheat, oat, and canola straws. *Biomass Bioenergy* **2014**, *60*, 58–67. [[CrossRef](#)]
6. Liu, Y.; Wang, J.; Wolcott, M.P. Assessing the specific energy consumption and physical properties of comminuted Douglas-fir chips for bioconversion. *Ind. Crops Prod.* **2016**, *94*, 394–400. [[CrossRef](#)]
7. Panainte, M.; Nedeff, V.; Burcă, G.; Savin, C.; Mosnegutu, E. Theoretical consideration regarding statistical calculus about distribution of size at particles at result from grinding process. *MOCM* **2004**, *10*, 83–88.
8. Cadoche, L.; Lopez, G.D. Assessment of size-reduction as a preliminary step in the production of ethanol from lignocellulosic wastes. *Biol. Wastes* **1989**, *30*, 153–157. [[CrossRef](#)]

9. Panainte, M.; Nedeff, V.; Moşneguţu, E. Analysis of grinding process at hammer mill. *MOCM* **2001**, *7*, 120–129.
10. Panainte, M.; Dasic, P.; Nedeff, V.; Mosnegutu, E.; Savin, C. Modalities to determine the energy consumption for the grindin gat vegetables product with variable texture. *MOCM* **2007**, *13*, 239–248.
11. Brennan, J.G. Food texture measurement. In *Developments in Food Analysis Techniques*; Elsevier Applied Science Publishers: London, UK, 1980; Volume 2.
12. Ragni, L.; Berardinelli, A. Mechanical behaviour of apples and damage during sorting a packaging. *J. Agric. Engng. Res.* **2001**, *78*, 78–91.
13. Panainte, M.; Nedeff, V.; Moşneguţu, E.; Savin, C.; Măcărescu, B.; Olaru, C. Determination of grinding energy to vegetable product through texture analysis method. *MOCM* **2007**, *3*, 128–134.
14. Adapa, P.; Tabil, L.; Schoenau, G. Grinding performance and physical properties of non-treated and steam exploded barley, canola, oat and wheat straw. *Biomass Bioenergy* **2011**, *35*, 549–561. [[CrossRef](#)]
15. Naimi, L.J.; Sokhansanj, S.; Bi, X.; Lim, C.J.; Womac, A.R.; Lau, A.K.; Melin, S. Development of size reduction equations for calculating energy input for grinding lignocellulosic particles. *Appl. Eng. Agric.* **2013**, *29*, 93–100. [[CrossRef](#)]
16. Karam, M.C.; Petit, J.; Zimmer, D.; Djantou, E.B.; Scher, J. Effects of drying and grinding in production of fruit and vegetable powders: A review. *J. Food Eng.* **2016**, *188*, 32–49. [[CrossRef](#)]
17. Indira, T.N.; Bhattacharya, S. Grinding characteristics of some legumes. *J. Food Eng.* **2006**, *76*, 113–118. [[CrossRef](#)]
18. Xiaoan, L.; Qinghong, L.; Fan, G.; Cong, H.; Peng, J.; Yonghua, Z. Effect of cutting styles on quality and antioxidant activity in fresh-cut pitaya fruit. *Postharvest Biol. Technol.* **2017**, *124*, 1–7.
19. Bitra, V.S.P.; Womac, A.R.; Chevanan, N.; Miu, P.I.; Igathinathane, C.; Sokhansanj, S.; Smith, D.R. Direct mechanical energy measures of hammer mill comminution of switchgrass, wheat straw, and corn stover and analysis of their particle size distributions. *Powder Technol.* **2009**, *193*, 32–45. [[CrossRef](#)]
20. Kratky, L.; Jirout, T. Modelling of particle size characteristics and specific energy demand for mechanical size reduction of wheat straw by knife mill. *Biosyst. Eng.* **2022**, *197*, 32–44. [[CrossRef](#)]
21. Panainte, M.; Moşneguţu, E.; Savin, C.; Nedeff, V. *Mărunţirea Produselor Agroalimentare*; Meronia, Rovimed Publishers: Bacău, Romania, 2005.
22. Panainte, M. Researches Regarding Optimizing the Grinding Process of Agrofood Products. Ph.D. Thesis, The “Gheorghe Asachi” Technical University of Iasi, Iaşi, Romania, 2008.
23. Ladan, J.N.; Shahab, S. Data-based equation to predict power and energy input for grinding wheat straw, corn stover, switchgrass, miscanthus, and canola straw. *Fuel Process. Technol.* **2018**, *173*, 81–88.
24. Wang, Y.L.J.; Barth, J.C.; Welsch, K.R.; McIntyre, V.; Wolcot, M.P. Effects of multi-stage milling method on the energy consumption of comminuting forest residuals. *Ind. Crops Prod.* **2022**, *145*, 111955.
25. Flumignan, D.L.; Rezende, K.A.; Comunello, E.M.; Fietz, C.R. Empirical methods for estimating reference surface net radiation from solar radiation. *Eng. Agricola* **2018**, *38*, 32–37. [[CrossRef](#)]
26. Saruchi, S.A.; Ariff, M.H.M.; Zamzuri, H.; Hassan, N.; Nurbaiti, W. Artificial neural network for modelling of the correlation between lateral acceleration and head movement in a motion sickness study. *IET Intell. Transp. Syst.* **2018**, *13*, 340–346. [[CrossRef](#)]
27. Paterson, C.; Clevers, H.; Bozic, I. Mathematical model of colorectal cancer initiation. *Proc. Natl. Acad. Sci. USA* **2022**, *117*, 20681–20688. [[CrossRef](#)] [[PubMed](#)]
28. Watanabe, S.; Kitawaki, T.; Oka, H. Mathematical equation of fusion index of tetanic contraction of skeletal muscles. *J. Electromyogr. Kinesiol.* **2010**, *20*, 284–289. [[CrossRef](#)] [[PubMed](#)]
29. Yu, Y.; Liu, J.X.; Zhang, K. Establishment of a prediction model for the cut size of turbo air classifiers. *Powder Technol.* **2014**, *254*, 274–280. [[CrossRef](#)]
30. Ageev, A.A.; Yakhontov, D.A.; Kadyrov, T.F.; Farakhov, M.M.; Lapteva, E.A. Mathematical equation of dispersed phase gas separation in a combined equipment. *Chem. Petrol. Eng* **2019**, *55*, 611–618. [[CrossRef](#)]
31. Hwang, D.H.; Han, J.H.; Lee, J.; Lee, Y.; Kim, D. A mathematical equation for the separation behavior of a split type low-shock separation bolt. *Acta Astronaut.* **2019**, *164*, 393–406. [[CrossRef](#)]
32. Ibyatov, R.I.; Kholpanov, L.P.; Akhmadiev, F.G.; Fazylyyanov, R.R. Mathematical modeling of phase separation of a multiphase medium. *Theor. Found. Chem. Eng.* **2006**, *40*, 339–348. [[CrossRef](#)]
33. Song, J.F.; Hu, X.F. A mathematical equation to calculate the separation efficiency of streamlined plate gas-liquid separator. *Sep. Purif. Technol.* **2017**, *178*, 242–252. [[CrossRef](#)]
34. Cobzaru, C.; Marinoiu, A.; Apostolescu, G.A.; Tataru-Farmus, R.E.; Cernatescu, C. Mathematical modeling for kinetics of Fe<sup>3+</sup> exchange on pretreated analcime. *Rev. Roum. De Chim.* **2019**, *64*, 403–407. [[CrossRef](#)]
35. Mosnegutu, E.; Panainte-Lehadus, M.; Nedeff, V.; Tomozei, C.; Barsan, N.; Chitimus, D.; Jasinski, M. Extraction of mathematical correlations applied in the aerodynamic separation of solid particles. *Processes* **2022**, *10*, 1234. [[CrossRef](#)]
36. Xxx, Stable Micro Systems. Available online: <https://www.stablemicrosystems.com> (accessed on 13 March 2020).
37. SYSTAT Software Inc. TableCurve 3D, Version 4.0. Available online: <https://systatsoftware.com/downloads/download-tablecurve-3d/> (accessed on 13 March 2020).